



UNIVERSITY OF LEEDS

This is a repository copy of *Segregation direction reversal of gas-fluidized biomass/inert mixtures – Experiments based on Particle Segregation Model predictions*.

White Rose Research Online URL for this paper:  
<http://eprints.whiterose.ac.uk/104603/>

Version: Accepted Version

---

**Article:**

Di Renzo, A, Di Maio, FP, Girimonte, R et al. (1 more author) (2015) Segregation direction reversal of gas-fluidized biomass/inert mixtures – Experiments based on Particle Segregation Model predictions. *Chemical Engineering Journal*, 262. pp. 727-736. ISSN 1385-8947

<https://doi.org/10.1016/j.cej.2014.10.028>

---

© 2014, Elsevier. Licensed under the Creative Commons Attribution-NonCommercial-NoDerivatives 4.0 International  
<http://creativecommons.org/licenses/by-nc-nd/4.0/>

**Reuse**

Unless indicated otherwise, fulltext items are protected by copyright with all rights reserved. The copyright exception in section 29 of the Copyright, Designs and Patents Act 1988 allows the making of a single copy solely for the purpose of non-commercial research or private study within the limits of fair dealing. The publisher or other rights-holder may allow further reproduction and re-use of this version - refer to the White Rose Research Online record for this item. Where records identify the publisher as the copyright holder, users can verify any specific terms of use on the publisher's website.

**Takedown**

If you consider content in White Rose Research Online to be in breach of UK law, please notify us by emailing [eprints@whiterose.ac.uk](mailto:eprints@whiterose.ac.uk) including the URL of the record and the reason for the withdrawal request.



[eprints@whiterose.ac.uk](mailto:eprints@whiterose.ac.uk)  
<https://eprints.whiterose.ac.uk/>

# Segregation direction reversal of gas-fluidized biomass/inert mixtures - experiments based on Particle Segregation Model predictions

Alberto Di Renzo<sup>\*,a</sup>, Francesco P. Di Maio<sup>a</sup>, Rossella Girimonte<sup>a</sup>, Vincenzino Vivacqua<sup>a</sup>

<sup>a</sup> Department of Environmental and Chemical Engineering, University of Calabria  
Via P. Bucci, Cubo 44A, 87036 Rende (CS), Italy

\* Corresponding author (A. Di Renzo): T.: +39 0984 496654, F.: +39 0984 496655; Email: alberto.direnzo@unical.it

## Abstract

The tendency for a gas-fluidized binary mixture to segregate or mix as a function of the size and density of the two solids, despite the extensive research efforts motivated by its strong influence on reactor performances, is still not fundamentally and thoroughly understood. Recently, the Particle Segregation Model (PSM) [1] has been proposed as a theoretical tool to predict the segregation direction of gently fluidized mixtures. An important and previously overlooked result, also predicted by PSM, is the presence of peculiar conditions in which the flotsam and jetsam components, for a given solid pair, may invert their role upon changing bed composition. In the present work, the segregation behavior of biomass/inert mixtures is investigated with the specific aim to check for the occurrence of this peculiar segregation direction reversal. Crushed olive pits are used as model biomass (1.54 mm diameter) in combination with glass beads (0.25 mm diameter) and two sand cuts (0.34 and 0.16 mm diameter). The segregation tendency of an initially mixed biomass/inert bed, deduced by the measured steady-state composition profiles, turns out to confirm the presence of segregation direction reversal as a result of a change of the relative solid volume fractions. Although the critical “equilibrium” composition is quantitatively captured only for the first pair, the occurrence of the phenomenon appears remarkably in agreement with the PSM predictions in all the three cases.

**Keywords:** Fluidization; Segregation; Biomass; Modeling; Mixing

**Type:** Research Article

## 1. Introduction

Bubbling fluidized beds in energy production/conversion units (combustion, gasification, etc.) often process a certain amount of large, less dense particulate material (the fuel) mixed with smaller, denser solids in the form of inert, heat or oxygen carrier. A solid catalyst or sorbent can also be present in the mixture to carry out specific tasks. In such processes, bed homogeneity (for processes requiring uniform properties, e.g. temperature) or controlled solid stratification (for sequentially combined operations, e.g. pyrolysis, gasification and CO<sub>2</sub> sorption) strongly influence the overall process efficiency [2,3]. However, controlled mixing or segregation can be hard to achieve in a bubbling bed [4–7]. The values of a long list of properties determine the mixing/segregation behavior of binary fluidized beds, including solids' size ratio and density ratio, gas superficial velocity, bed composition, rendering its characterization particularly complex.

Experimental investigation of the segregation tendency in binary bed was carried out by many research groups. Historically, the most significant contributions have been proposed by Rowe and co-workers [8–10]. The minimum fluidization velocities of multicomponent beds have been studied extensively by looking at the effect of particle size difference [11–17], density difference [18,19] or both [20–26]. Analogously, several numerical simulations using different approaches have supplemented these in the interpretation of the observations, see e.g. [27–35].

According to the nomenclature proposed by Rowe et al. [8], a component is termed flotsam if upon fluidization it tends to float to the bed surface and jetsam if it tends to sink to the bottom. The main effects can be summarized by a few well-established trends. The rest being equal, the dependence of the drag force on the projected particle surface determines that larger/smaller spheres tend to act as jetsam/flotsam, respectively. Denser solids tend to sink to the bottom while less dense solids are typically found segregated up to the bed surface. The effect of the gas-velocity is to intensify bed agitation due to increased bubbling. Therefore, higher-velocity fluidized beds tend to reach a more uniform, mixed state. The mixing degree achieved depends on the segregation tendency of the mixture. For example, with solids of significant density difference the velocity required to contrast the strong segregation can easily exceed the value sufficient to elutriate the lighter component and full mixed cannot be achieved. It is also known that the relative proportions of the components can also influence the packed bed voidage, thereby affecting the minimum fluidization velocity of the mixture, while its direct effect on mixing and segregation is not yet clear.

The combination of properties driving towards opposed tendencies can lead to an unpredictable behavior. It is common to consider that density difference typically prevails over size difference.

However, if the finer solid is sufficiently fine a point will be reached in which the denser component acts as flotsam, as observed a few decades ago by Chiba et al. [36]. It can be shown that, in general, when the effect of size difference counteracts that of the density difference, even the basic question of which one component does act as flotsam in the mixture is not at all trivial. Not only is the role of the two components largely unpredictable, but also whether or not other variables can change this role is unclear. As an example, a change of superficial velocity or bed composition determines the well-known layer inversion phenomenon in binary liquid-fluidized beds, as copiously documented in the literature [37–40], but no corresponding phenomena have been investigated yet in gas-fluidized beds. Reference to the suspension condition of the pure components via a comparison of their minimum fluidization velocities (discriminating the packed from the fluidized component) has no theoretical foundation, as the two solids are known to behave rather differently in the mixture than as pure. Indeed, it will be recalled below that identification of the flotsam component results from a different theoretical perspective. The problem of attributing the roles of flotsam and jetsam, which we call the determination of the segregation direction, has been addressed by our group in recent works [1,41], which led to the development of the so-called Particle Segregation Model (PSM). A comprehensive list of experimental data exhibiting segregation in both directions essentially corroborated the parameter-free predictions of PSM. Still, in some cases source data were incomplete or the extent of the segregation process and the condition of mixing were difficult to assess. On the other hand, by guiding specific experimentation, PSM predictions offer a new and more direct possibility to validate the results, an opportunity that inspired the work discussed below.

The main aim of the present study is to report on the PSM-guided observation of segregation direction reversal in binary gas-fluidized beds as a result of a change of bed composition. Gentle fluidization of three initially mixed fluidized systems, consisting of different amounts of biomass particles combined with two sand cuts and one cut of glass ballotini, was considered. Starting from the PSM predictions, the sizes of the inert solids were selected in order for the mixture to exhibit a change of segregation direction with bed composition, at least according to PSM predictions. With such solids mixtures, experimental tests were carried out to investigate the actual occurrence of the peculiar phenomenon and verify the PSM predictions.

The Particle Segregation Model approach and relevant results will be presented in the following Section. The experimental methods and materials used will then be described, detailing how the PSM predictions guided the selection of the inert size. Segregation experiments and results of the observed evolution of the concentration profile in the bed will be finally presented and discussed.

## 2. The Particle Segregation Model (PSM)

In the study of the segregation phenomena occurring in initially mixed beds upon fluidization, it is important to determine the prevalence of the effect of either size or density of the involved solids. In the case of binary systems composed of small, dense particles mixed with big, less dense particles, it is not simple to predict whether or not segregation will take place and if so which one of the two components will tend to float or sink. In order to tackle this problem, in the Particle Segregation Model [1,41] it is proposed to compare the weight with the upward hydrodynamic force acting on one particle of a given species immersed in the fully mixed bed, assuming it at suspension conditions (Figure 1). Note that other forces, like particle-particle drag or contact interactions, are not considered here, as only the initial unbalance of force driven by the action of the fluid on each separate species is investigated.

Without loss of generality, the small component is denoted as species 1 and the bigger component as species 2. If the bigger component tends to segregate upwards, the relevant force unbalance along the vertical coordinate should be described by the following inequality::

$$\rho_2 \pi \frac{D_2^3}{6} g < W_2 |_{\bar{u}_s} \quad (1)$$

where  $\rho$  and  $D$  are the particle density and size, respectively,  $g$  is the gravitational acceleration. The term on the right-hand side is the total hydrodynamic force  $W$  acting on the particle at a gas superficial velocity for which the entire (mixed) bed is fluidized,  $\bar{u}_s$ , i.e. at conditions where the overall bed weight is supported by the action of the gas flow. The other segregation direction is obtained if the opposite sign applies in Eq. (1). In the following, a solution will be searched for Eq. (1) in the form of equality, as the relation discriminating between the two segregation directions.

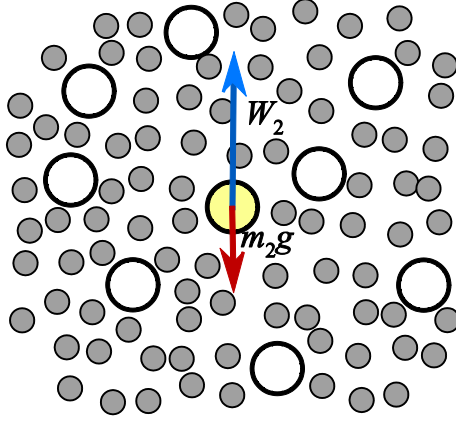


Fig. 1. Scheme of the force balance on a particle in a binary mixture.

In dense systems, such force is often conventionally decomposed into a fluid pressure gradient force and a term  $F$  explicitly dependent on velocity, named drag,

$$W_2|_{u_s} = -\pi \frac{D_2^3}{6} \nabla P + F_2|_{u_s} \quad (2)$$

It is worth noting that such decomposition is only formal, arisen from recognizing the similarity with liquids and useful for computing the two terms more easily. Indeed, the pressure gradient appearing in Eq. (2) in general refers to a scale that is much bigger than the particle size, possibly the entire scale of the system (so that it becomes measurable). Therefore, such concept is not to be confused with the local pressure gradient around the particle surface, a datum that has become available in more recent years, e.g. thanks to resolved CFD simulations of the flow through particle systems. When such data are available, the value necessary here can be obtained from the detailed results provided filtering to an appropriate scale is adopted.

The pressure gradient force is composed of an Archimedean term due to gas density and a generalized buoyancy force due to the fact that the gas supports the other particles

$$-\nabla P = \rho g - \nabla p \quad (3)$$

It is the second term in the right-hand side of Eq. (3) that is responsible for the unrecoverable pressure loss across the bed [42]. By denoting  $-\nabla p$  as net pressure gradient, the net fluid particle force  $N$  acting on species 2 can be defined

$$N_2|_{u_s} = -\pi \frac{D_2^3}{6} \nabla p + F_2|_{u_s} \quad (4)$$

and used in Eq (1) in place of  $W_2$ , at least for the present case of gas-fluidized beds.

Recalling that suspension conditions are being assumed for the initially mixed bed, the pressure gradient across the bed can be easily computed from the total bed weight per unit volume

$$-\nabla p = \bar{\rho}(1 - \varepsilon)g \quad (5)$$

where  $\bar{\rho} = x_1\rho_1 + (1 - x_1)\rho_2$  is the solid density averaged by the solids' volume fractions  $x$  and  $\varepsilon$  is the bed voidage.

The most demanding task is to be able to express correctly the drag force acting on a particle immersed in a binary mixture. The following formulation, derived originally by van der Hoef et al. [43], is selected mainly because of its simplicity, despite various improvements or other possibilities exist, see e.g. [44–47]. It provides the following direct expression that relates the force acting on a particle of one species to the average drag force in the system

$$F_2 = y_2^2 \bar{F} \quad (6)$$

where

$$y_i = \frac{D_i}{\bar{D}} \quad (7)$$

$$\bar{F} = \sum_i \frac{x_i}{y_i^3} F_i \quad (8)$$

and the average diameter is Sauter's mean definition  $\bar{D} = \left( \sum_i \frac{x_i}{D_i} \right)^{-1}$ .

Because of the assumption of fluidized conditions, instead of calculating the average drag force in terms of velocity, voidage, etc. the same is obtained by evaluating the suspended weight of one (equivalent average) particle. Elaboration of Eq. 5 in order to expand the left-hand side in terms of the contributions of each species yields:

$$\frac{6}{\pi} \frac{1 - \varepsilon}{\varepsilon} \sum_i \frac{x_i F_i}{D_i^3} = \bar{\rho}(1 - \varepsilon)g \quad (9)$$

With the definitions of the average force  $\bar{F}$  (Eq. 7) and the polydispersion index  $y_i$  (Eq. 8), the average force is:

$$\bar{F} = \bar{\rho} \frac{\pi}{6} \bar{D}^3 g \quad (10)$$

As a consequence, the explicit calculation of the gas superficial velocity required for suspension is not necessary. Similarly, no specification of the flow regime is required, i.e. the result shall apply to any flow condition. The only assumption is for the bed to be fully suspended by the fluid. Also, since Eq. (1) is applied essentially in the emulsion phase, bubbles are assumed not to play a dominant role. Such conditions are realized for a homogeneously mixed bed using gentle

fluidization and at the beginning of the observations. Indeed, once segregation takes place the overall results discussed here are no longer directly applicable, because a gradually different concentration develops along the axis and the corresponding force balance should be adapted. The situation is complicated by the fact that part of the bed may undergo defluidization as a result of segregation, making the drag-weight balance inapplicable in those regions.

By using the results obtained in Eqs (4, 6 and 10), the explicit form of Eq. (1) is

$$\rho_2 \frac{\pi}{6} D_2^3 g = \bar{\rho}(1-\varepsilon) \frac{\pi}{6} D_2^3 g + \varepsilon \bar{\rho} \frac{\pi}{6} D_2^2 \bar{D} g \quad (11)$$

or

$$\bar{s} = 1 - \varepsilon + \varepsilon \bar{d} \quad (12)$$

in which the following definitions apply

$$\bar{s} = \frac{\rho_2}{\bar{\rho}} \quad (13)$$

$$\bar{d} = \frac{\bar{D}}{D_2} \quad (14)$$

The result expressed by Eq. (12), cast as a function of the following species-to-species density and size ratios, respectively,

$$s = \frac{\rho_2}{\rho_1} \quad (15)$$

$$d = \frac{D_1}{D_2} \quad (16)$$

reads

$$s = \frac{(1-d)(1-\varepsilon)x_1 + d}{(1-x_1)[\varepsilon + (1-\varepsilon)d] + x_1} \quad (17)$$

Fig. 2 shows the equilibrium lines at different compositions that separate the two areas of the density vs. size ratio chart characterized by a different behaviour at fixed values of the bed voidage. It is worth noting that the formulation of Eq. (17) provides the possibility of including the dependence of voidage on composition, as commonly observed in binary packed mixtures. However, Fig. 2 shows that the effect of different voidage values, typically heavily impacting on fluidization properties, is relatively limited on the segregation equilibrium lines.

While expressions of the form of Eq. (12) have been presented and discussed previously [1,41], the general derivation in terms of the weight of the average particle is new. Particularly relevant is the

fact that no specific form of the explicit dependence of the hydrodynamic force on voidage or velocity is required (not even mention of the flow regime established). Nor is an expression of the average minimum fluidization velocity necessary in order to proceed.

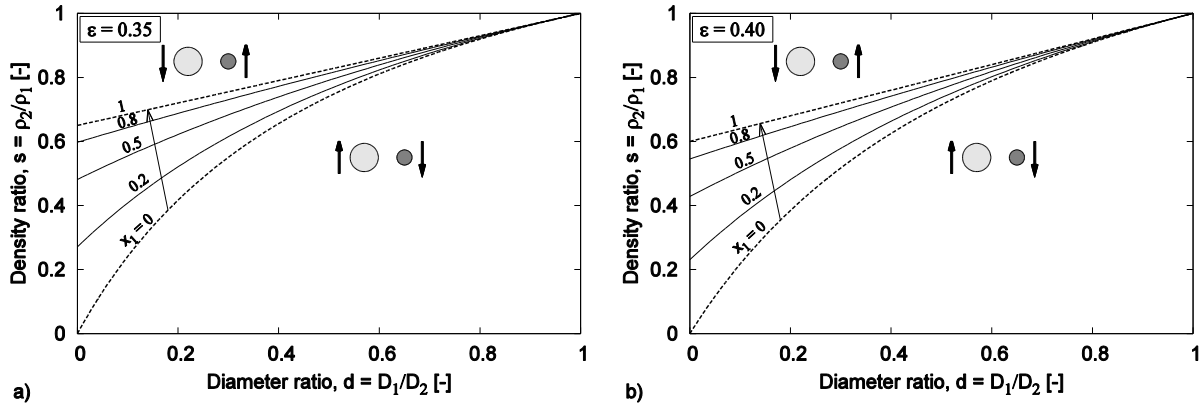


Fig. 2. Segregation equilibrium lines and species behaviour in terms of density ratio vs. size ratio.

Various bed compositions are shown in the plots for voidage values 0.35 (a) and 0.40 (b).

## 2.1 Discussion of the PSM results

The inherent concept behind Eq. (12) is essentially that when the binary mixture is suspended as a whole, so an average particle would be at mechanical equilibrium, the individual species (2 in this case) is not necessarily at equilibrium. Segregation would then result from this unbalance and its direction can be straightforwardly predicted by comparing the relevant forces.

In practical uses, note that Eq. (17) expresses a comparison of the forces acting on a particle of species 2, named its weight, on the LHS, and the hydrodynamic force, on the RHS. Consequently, if the value of  $s$  is greater than the value of the RHS then at overall equilibrium particles of species 2 will be pushed downwards by the action of gravity, so species 2 will tend to settle to the bottom of the bed (acting as jetsam). Conversely, lower values of  $s$  correspond to conditions where species 2 would tend to float, appearing as flotsam. Considering the equilibrium of the total bed, the mechanical condition of species 1 is specular to that of species 2.

If the value of  $s$  is equal to the RHS of Eq. (17), the condition of equilibrium will apply to both the overall bed and the individual species, determining a condition in which the initial mixed (packed) bed will maintain the degree of mixing upon fluidization. Such implication could provide interesting alternatives in processes where segregation is contrasted by using high fluidizing gas velocities with the sole purpose of producing a vigorous bubbling regime.

The presence of a segregation equilibrium condition prescribed by Eq. (17) implies the possibility, for selected systems of given sizes and densities, to cross it by changing the solid composition. As a result, the segregation direction initially exhibited at low (or high) concentrations should revert to the opposite one at high (or low) concentrations. A set of experimental tests will be described in the following sections in order to check for the occurrence of this segregation reversal.

### **3. Materials and experimental procedure**

The experimental set-up was composed of a 9.3 cm ID Perspex cylindrical fluidization column, equipped with a 4 mm thick plastic porous distributor. Air at ambient conditions was the fluidizing medium, whose flow from a compressor can be regulated by a set of rotameters. A pressure probe located just above the distributor, connected to a water manometer, was used to measure the air pressure drop across the particle bed.

The mixtures investigated involved different compositions of biomass particles combined with three inert solids, as typical representations of fuel/inert industrial charges. Biomass was available in form of dried, crushed olive pits (OP), while glass ballotini and sand were used as inert. The original biomass stock was highly polydisperse and had a relatively large size. Sieving in the range 1.4–2 mm was necessary to bring the sample within workable diameters. Inert particles (glass ballotini, GB, and two sizes of sand granules, SG) were available in different cuts, and their final sizes were selected in order for the resulting mixture to fall within the area of Fig. 2, where reversal with bed composition is predicted to occur, possibly with a critical composition of the order of  $x_1 = 0.5$ . Fig. 3 shows a photograph of the biomass and glass ballotini. Owing to the uncertainties related to the irregular shape, a determination of the biomass hydrodynamic average size through pressure drop measurements was carried out. Fig. 4 shows the fluidization curve of the biomass sample. The fixed bed data have been used in combination with Ergun's equation to find the appropriate value of the average size, resulting in  $D_{OP1540} = 1.54$  mm. The properties of the examined materials, including the experimentally determined  $u_{mf}$ , are summarized in Table 1.



Fig. 3. Photograph showing representative samples of the biomass particles (OP1540) on the left and the glass ballotini (GB0250) on the right.

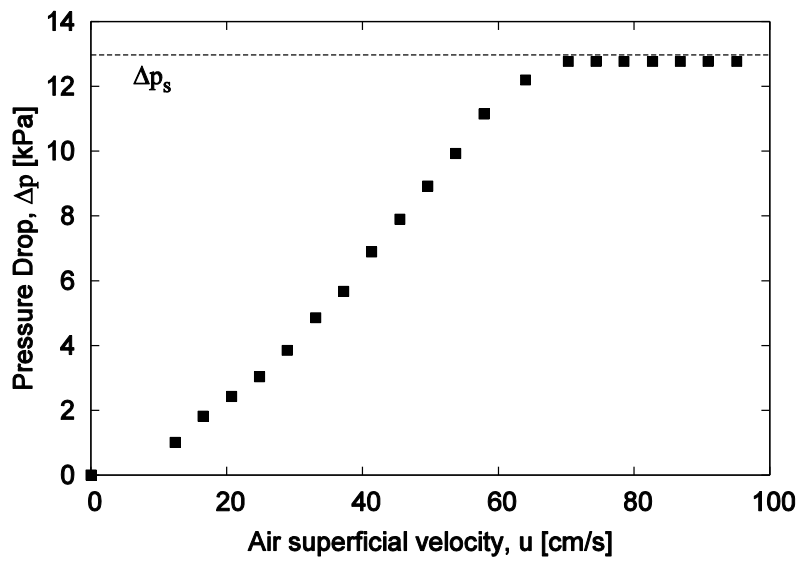


Fig. 4. Fluidization curve of the biomass (OP1540). The dashed line represents the theoretical pressure drop at bed suspension  $\Delta p_s$  (bed weight/cross section area).

Table 1. Properties of the solids.

Solid	Identifier	$\rho$ [kg/m <sup>3</sup> ]	D [mm]	$u_{mf}$ [cm/s]
Olive pits (biomass)	OP1540	1380	1.54	66.1
Glass ballotini	GB0250	2480	0.25	6.6
Sand granules	SG0340	2590	0.34	22.8
---	SG0160	2590	0.16	5.6

### 3.1 Experimental procedure

Fluidization tests involving binary beds were all performed starting from an initially mixed bed. Care was taken to ensure the maximum bed homogeneity by composing the required total mass with layers by layers, for each one mixing appropriate amounts of the two solids. Gentle pouring into the column was carried out by means of a funnel connected to a long tube in order to prevent segregation during the fall and ensure high reproducibility. In selected cases, the effective composition uniformity throughout the column was checked right after pouring, following the procedure described below for the axial composition profile. Bed heights were such as to obtain a bed-height-to-diameter aspect ratio of about 1.7 in all tests. Bed voidage measurement was obtained using the data of the loaded mass of the two components and bed height at the different compositions. Fluidization tests were carried out according to the following procedure: initially the air superficial velocity was slowly increased with the bed in the packed state; the velocity at which the bed entered the suspended state (the initial fluidization velocity) was recorded; the gas velocity was further increased progressively, in order to ensure a reasonable bed mobility with a relatively quick attainment of the steady-state composition profile, up to a value 30 to 50% higher than the initial fluidization velocities and was then kept constant for the test (see Table 2). At each desired velocity, typically three to five minutes were sufficient to reach a condition where the solid layers formed did not show any further dislocation. Measurements of the concentration profiles in the column were obtained after “freezing” the bed (i.e. shutting the gas flow suddenly); then, horizontal layers of particles, about one centimeter thick, were withdrawn from the top of the column, separated by sieving in the two cuts, each one weighed, in order to reconstruct the volumetric fraction profile along bed height. Each test was repeated twice and in a few cases three times and reported data are the average values.

## 4. Results and discussion

The current investigation aims primarily at verifying the peculiar behavior of the segregation direction reversal. This task is accomplished in both qualitative and quantitative terms, i.e. the occurrence of the phenomenon, which – it is to remark – has never been reported and investigated explicitly in the literature, is checked first; then, examination of the steady-state concentration profiles at various nominal compositions will allow comparing the observed versus predicted critical reversal conditions quantitatively.

Three combinations of the solids listed in Table 1 were investigated at different initial bed compositions. The solid mixtures considered are listed in Table 2, along with their properties. All

the resulting density and size ratios correspond to systems predicted to exhibit a change of segregation direction as a function of bed composition (Fig. 5). The compositions investigated, the corresponding gas superficial velocities and the critical volume fractions of species 1, as predicted by Eq. (17) at  $\varepsilon = 0.4$ , are reported in Table 2. Note that the location of the points A-C on the density-size ratio chart (Fig. 5), which incidentally are independent of the mixture composition and bed voidage, also allows estimating the corresponding critical values  $x_{1,eq}$ , at least for the selected voidage value used to draw the equilibrium lines. For each of the three mixtures the dependences with composition of voidage, expected equilibrium density ratio and composition profiles are investigated.

Table 2. Binary mixtures investigated.

Mixtures (inert-biomass)	GB0250-OP1540	SG0340-OP1540	SG0160-OP1540
System identifier	A	B	C
$d = D_1/D_2$ , [-]	0.16	0.22	0.10
$s = \rho_2/\rho_1$ , [-]	0.56	0.53	0.53
$x_1$ , [-]	0.1, 0.2, 0.3, 0.4, 0.6, 0.8	0.1, 0.2, 0.3, 0.4, 0.5, 0.6, 0.7, 0.8, 0.9	0.1, 0.2, 0.3, 0.4, 0.5, 0.6, 0.7, 0.8
$u_{exp}$ for each $x_1$ , [cm/s]	40.8, 20.4, 12.2, 5.3, 4.7,	51.3, 42.5, 37.7, 32.3, 28.1,	41.1, 29.0, 21.8, 16.9, 13.6,
	4.9	27.5, 26.9, 24.5, 21.1	11.8, 10.7, 10.8
$x_{1,eq}$ for $\varepsilon = 0.4$ (Eq. 17), [-]	0.51	0.29	0.57

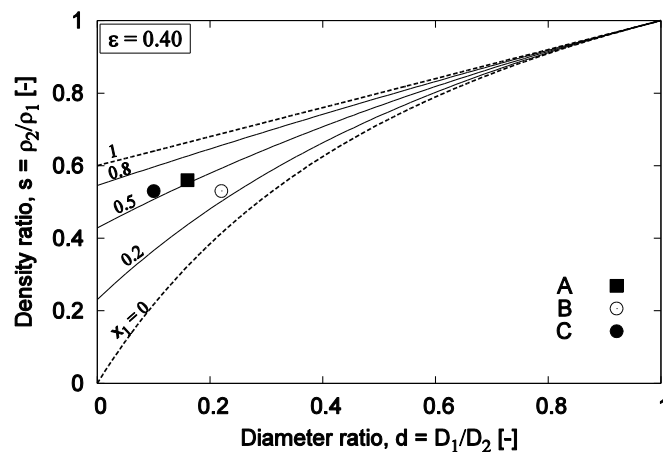


Fig. 5. Location of the systems A to C of Table 2 on the density ratio vs. size ratio chart. Lines represent equilibrium conditions at  $\varepsilon = 0.4$  and the compositions shown.

#### 4.1 System A: GB0250-OP1540

In the first mixture (A) biomass particles are the larger, less dense species and spherical glass ballotini act as smaller, denser inert. In consideration of the significant difference in size, the bed voidage of the binary mixture can be considerably different than that exhibited by the two individual constituents. Fig. 6a shows the observed dependence of the bed voidage on the volume fraction of the glass ballotini. As typically observed, while the individual components pack at around  $\varepsilon = 0.4$ , the voidage of the mixture decreases at the intermediate compositions, showing a minimum value  $\varepsilon = 0.28$  for  $x_1 = 0.4$ . As shown in Fig. 2, such effect can have an impact on the equilibrium lines, so a recalculation of each curve at the appropriate voidage should be performed. The impact of the actual voidage on the critical reversal conditions can also be assessed by comparing the critical

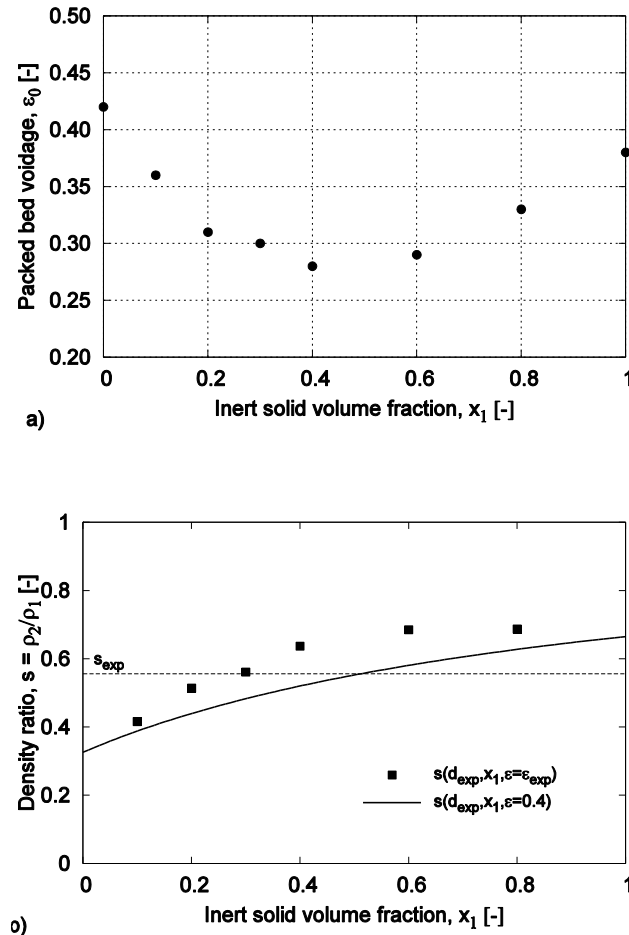


Fig. 6. Dependence of bed voidage on the volume fraction of the inert particles (a) and comparison (b) of the solids' density ratio  $s_{\text{exp}}$  (dashed line) with the density ratio  $s$  computed by the PSM equilibrium Eq. (17) using a constant voidage  $\varepsilon = 0.4$  (solid line) and the experimental profile  $\varepsilon_{\text{exp}}$  (symbols). System A: GB0250-OP1540 with properties listed in Tables 1 and 2.

density ratio for a given size ratio at various bed compositions. Fig. 6b shows the dependence of the critical value of  $s$  for the size ratio of mixture A computed by means of Eq. (17) both using an approximate value of  $\varepsilon = 0.4$  (solid line) and using the appropriate value of the voidage at each composition (symbols). The intersection with the value of the actual density ratio ( $s_{exp}$  in the chart) yields the critical equilibrium composition  $x_{1,eq}$  on the abscissa. It can be observed that the significant variation of the voidage in the mixture reflects in an appreciable shift of the critical  $x_1$  when the actual voidage is taken into account. With respect to the datum reported in Table 2, a more correct estimate of the critical composition appears to be around  $x_1 = 0.3$ .

Measurements of the steady-state volumetric fraction profiles of the glass ballotini along bed height are reported in Fig. 7. For each test, the observed composition profiles are reported together with vertical lines showing the nominal (i.e. overall) bed composition. Note that each vertical line also identifies an ideally mixed system, i.e. the initial state of the bed. The comparison of the local volume fraction with the nominal value allows the segregation direction to be qualitatively assessed and the presence of the reversal condition to be identified quantitatively.

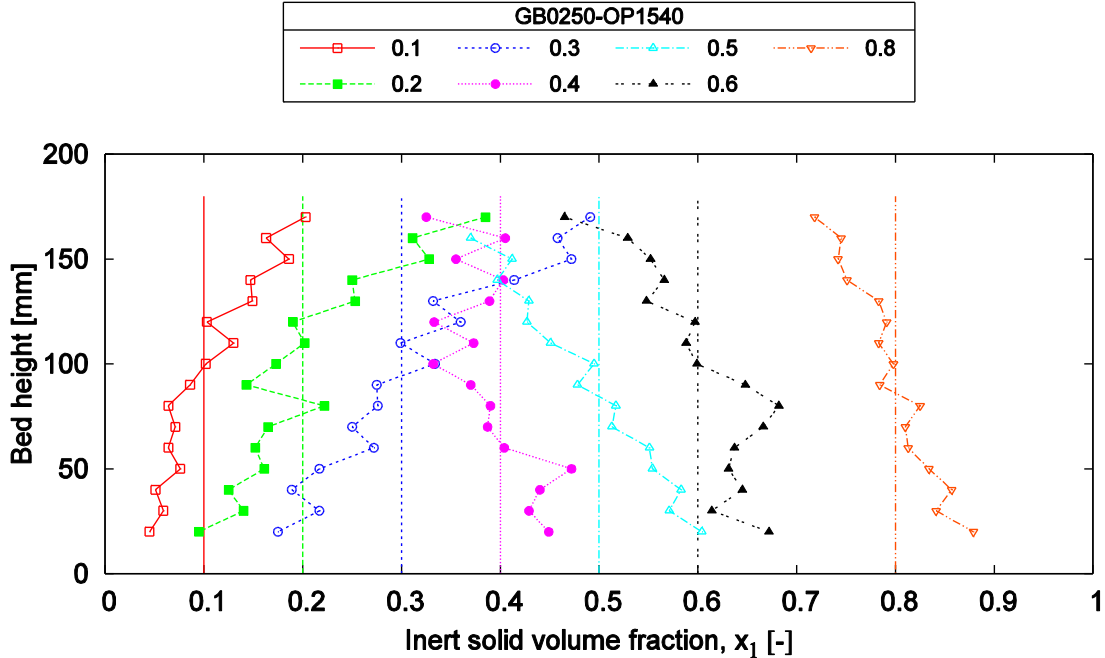


Fig. 7. Steady-state composition profiles along bed height. Actual measured profiles (lines with symbols) are shown with different colours for each test, together with a vertical line identifying the overall bed composition. System A: GB0250-OP1540 with properties listed in Tables 1 and 2.

For the system A, the composition profiles shown in Fig. 7 appear relatively close to the nominal fraction of the species, denoting systems in all cases not too far from a condition of mixing. However, by looking at the profiles as they change with the nominal composition, it can be observed that a segregation direction reversal is rather evident. At compositions up to  $x_1 = 0.3$  there is a prevalence of the glass ballotini in the upper portion of the bed. On the contrary, for volume fractions of  $x_1 = 0.5$  or higher, it is the biomass that prevails in the upper layers of the fluidized bed, acting as flotsam. For a volumetric fraction  $x_1 = 0.4$ , essentially mixed layers are found throughout the bed. Interestingly, not only is the segregation reversal observed in the examined range of compositions, but the equilibrium condition turns out to occur at an inert solid volume fraction in remarkable agreement with the predictions of Eq. (17).

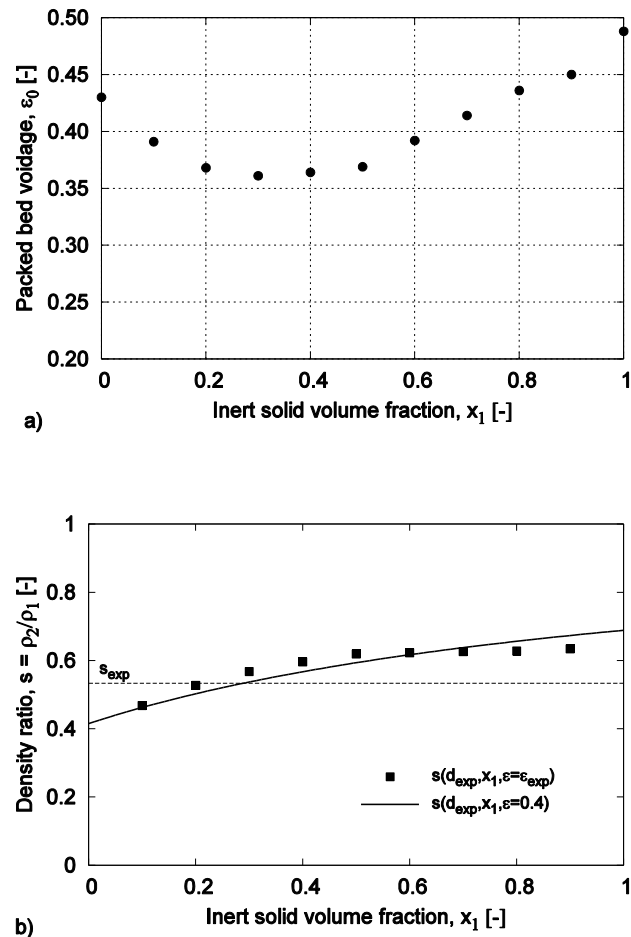


Fig. 8. Dependence of bed voidage on the volume fraction of the inert particles (a) and comparison (b) of the solids' density ratio  $s_{exp}$  (dashed line) with the density ratio  $s$  computed by the PSM equilibrium Eq. (17) using a constant voidage  $\epsilon = 0.4$  (solid line) and the experimental profile  $\epsilon_{exp}$  (symbols). System B: SG0340-OP1540 with properties listed in Tables 1 and 2.

## 4.2 System B: SG0340-OP1540

Mixture B is composed of biomass particles and the larger cut of sand granules. As in all other cases, the inert solid is denser and smaller than the fuel particles. The size ratio is less extreme than the other two systems. Consequently, the change of voidage with composition is more limited in span (see Fig. 8a). The minimum voidage value is  $\varepsilon = 0.36$  for  $x_1 = 0.3$ . It is noteworthy that the voidage of the pure sand granules is relatively high, approaching almost 0.5, probably owing to the non-spherical shape of the granules. This also explains the increase of the packed bed voidage of sand-rich mixtures well above  $\varepsilon = 0.4$ .

According to the datum in Table 2, the segregation reversal condition should be attained around  $x_1 = 0.29$ . Opposite to the observations for system A, taking into account the variation of voidage does not imply a significant shift of the critical density ratio and, consequently, the critical reversal composition (Fig. 8b). Interpolating between two successive points, intersection with the actual value of the density ratio  $s_{exp}$  yields a critical composition below  $x_1 = 0.23$ .

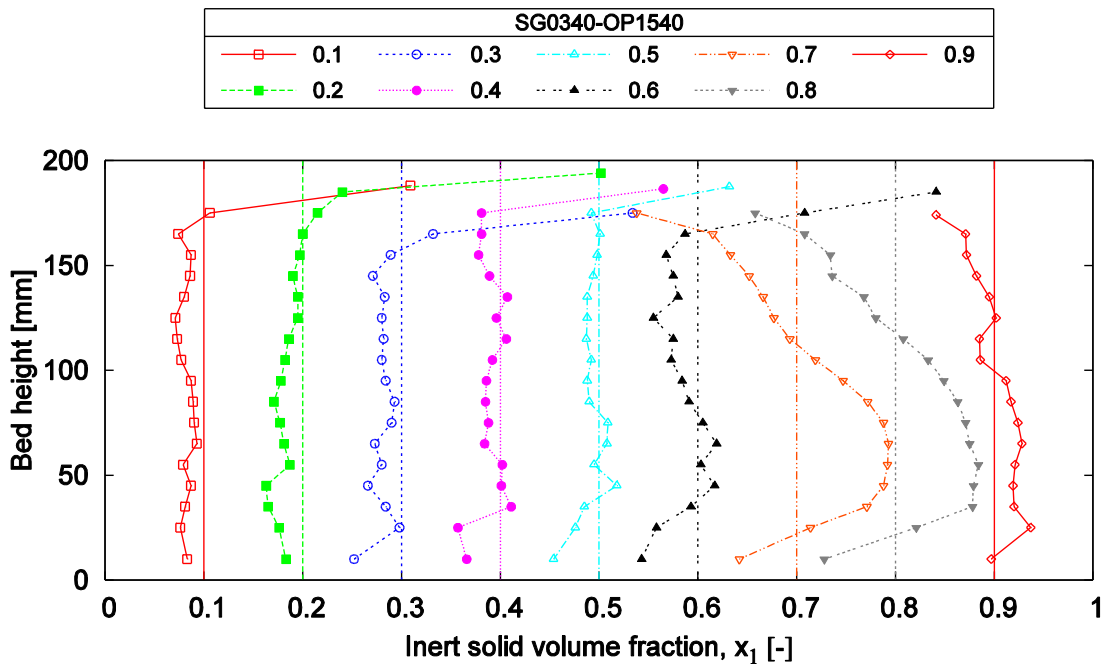


Fig. 9. Steady-state composition profiles along bed height. Actual measured profiles (lines with symbols) are shown with different colours for each test, together with a vertical line identifying the overall bed composition. System B: SG0340-OP1540 with properties listed in Tables 1 and 2.

Composition profiles of the sand granules along bed height for system B are shown in Fig. 9. In many plots a significant part of the profiles is in the close vicinity of the nominal composition, again witnessing a partly homogeneous, mixed bed. This is particularly true for profiles at volume fraction up to about  $x_1 = 0.6$ , for which the bed manifests an upper, shallow portion enriched in sand particles withdrawn from the essentially uniform rest of the bed. For volume fractions of about  $x_1 = 0.7$  and higher, the composition profiles change significantly their shape, exhibiting an upper part of the bed rich in biomass. The extent of prevalence of the biomass particles decreases progressively moving deeper until, slightly above the middle of the bed, the profiles cross the nominal composition. Sand granules show an appreciable dominance in the lower half of the bed even for nominal compositions as extreme as  $x_1 = 0.9$ . An exception is the very last solid layer at the bottom, at all concentrations enriched with biomass particles. Rather than to the influence of unpredicted factors, such phenomenon is likely attributable to distributor effects.

The profiles in Fig. 9 prove the occurrence of a segregation reversal condition also for system B. However, in comparison with the results found for system A, the quantitative prediction of the critical composition by means of Eq. (17), even with the correct voidage, appears much less reliable.

#### 4.3 System C: SG0160-OP1540

In mixture C biomass is coupled to a finer cut of sand granules. The size ratio, nearly 1 to 10, in this case is rather extreme and the possibility for the fine sand to percolate through the biomass particles rendered the experimental investigation more complex. It is the case to mention that it was not possible to leave the solids, even packed and without air flow, in the initial, fully-mixed state for more than a few minutes, as the sand particles tended naturally to sink, flowing slowly through the interstices among the bigger biomass particles. Experimental difficulties prevented us from being able to examine mixtures at very high fractions of sand, e.g.  $x_1 = 0.9$ .

Similar to the previous cases, the bed voidage exhibits a significant dependence on composition, as shown in Fig. 10a. A minimum voidage value of  $\varepsilon = 0.32$  was found for a volume fraction of sand of  $x_1 = 0.3$ . Similar to SG0340, also the pure finer sand SG0160 exhibits a packed bed voidage as high as about  $\varepsilon = 0.48$ . The determination of the critical composition for segregation reversal can be performed based on the data plotted in Fig. 10b. The theoretical condition for segregation equilibrium, including voidage-composition effects, is predicted to occur at about  $x_1 = 0.4$ .

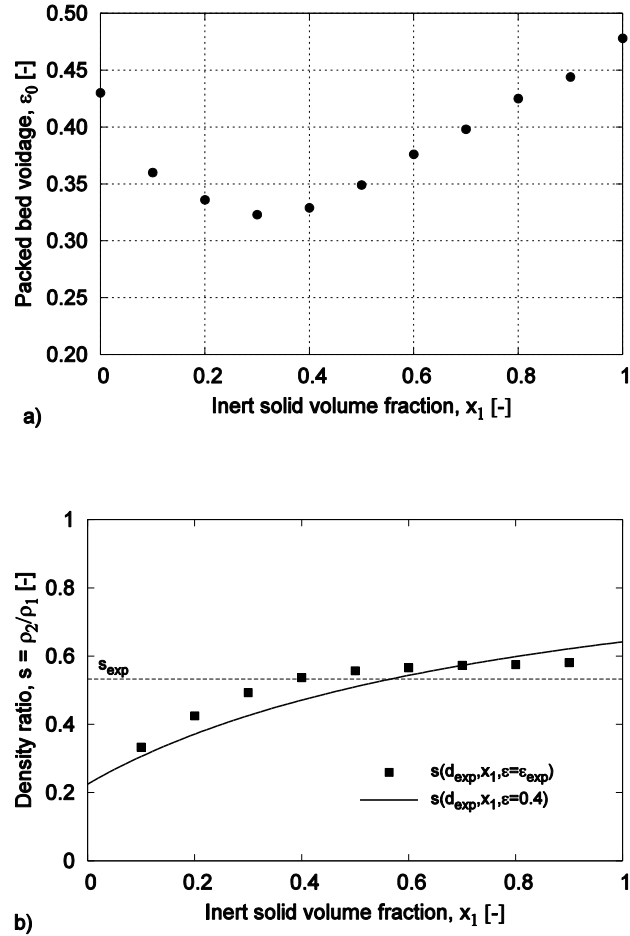


Fig. 10. Dependence of bed voidage on the volume fraction of the inert particles (a) and comparison (b) of the solids' density ratio  $s_{exp}$  (dashed line) with the density ratio  $s$  computed by the PSM equilibrium Eq. (17) using a constant voidage  $\epsilon = 0.4$  (solid line) and the experimental profile  $\epsilon_{exp}$  (symbols). System C: SG0160-OP1540 with properties listed in Tables 1 and 2.

By looking at the composition profiles of Fig. 11, it can be noted that the presence of an extreme size ratio leads to a stronger tendency towards segregation. The fine sand tends to stratify to the top of the bed right from the lowest compositions investigated, creating a nearly pure layer at volume fractions between  $x_1 = 0.4$  and  $0.6$ . At higher values, the upper layer shows a slight decrease of the fraction of fines, and the upper portion of the profile shows an inverted profile, with a decreasing fraction of sand particles with bed height. This result is more clearly observable at  $x_1 = 0.8$ . Although it is less than a clear manifestation of a direction reversal, it is quite evident that a change of segregation pattern occurs at the higher volume fractions ( $x_1 \geq 0.8$ ) with respect to the lower values also for this system. Unfortunately, the analysis is complicated by the fact that the fluidization process occurs starting from the bottom of the bed rather than from the top. As soon as the bed is suspended, the (packed) upper part of the bed is lifted as a lump by the (fluidized) lower section of the bed.

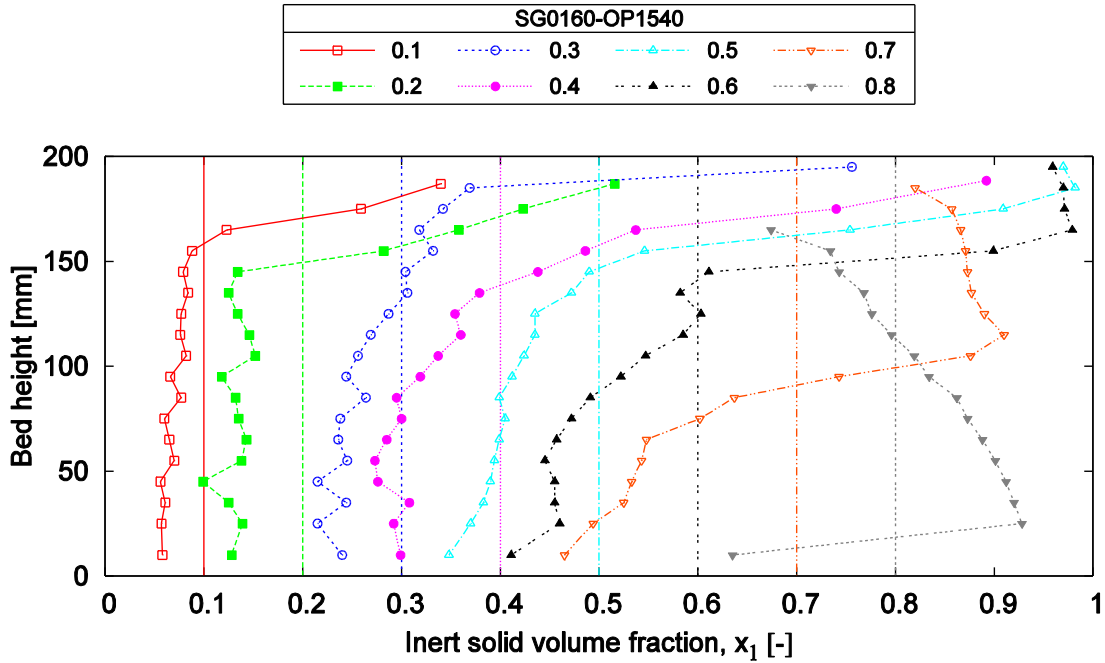


Fig. 11. Steady-state composition profiles along bed height. Actual measured profiles (lines with symbols) are shown with different colours for each test, together with a vertical line identifying the overall bed composition. System C: SG0160-OP1540 with properties listed in Tables 1 and 2.

Quantitative comparison of the segregation reversal point for system C, that can be estimated roughly at about  $x_1 = 0.7$ , as compared to the predicted critical volume fraction of  $x_1 = 0.4$  shows that the simplified approach of the PSM in this case would appear useful only to provide estimates.

#### 4.4 Discussion

The experimental observations presented in the previous subsection provide a set of data that substantiate the hypothesis that gas-fluidized beds can exhibit segregation reversal with bed composition and that this can be easily predicted, if not quantitatively at least qualitatively, by applying the Particle Segregation Model relationship.

Before discussing the implications of such results, it is instructive to recall some concepts previously used to distinguish between flotsam and jetsam components. In the absence of a reliable theoretical model, the commonly established rule that the denser component is always jetsam is typically adopted. Indeed, it is known that with binary fluidized beds the density difference dominates over size difference. However, it is also true that in the case of a denser, but much smaller component, the consideration mentioned above that density effects prevail over size effects

must at some point break; otherwise, one should imagine that a tiny powder of a metal should sink when fluidized along with e.g. big ceramic balls. So, in case of “complex” mixtures for which the simple density rule cannot be judged reliable, one may be tempted to attribute the role of flotsam or jetsam by comparing the minimum fluidization velocity of the two individual components. As shown in previous works [1,41], the results of this assumption do not agree with many experimental observations, including the ones discussed here (see Table 1). Additionally, none of the previous criteria include even the possibility of a change of segregation direction with composition, which is the main result of the presented experimental investigation.

It is from this perspective, i.e. the previous lack of tools in this field, that one should assess the applicability of the PSM results to binary bubbling beds. Considering the number and significance of the approximations in the derivation, the very simple mathematical form of the Particle Segregation Model and the lack of fitting parameters, it is quite remarkable that the predictions of segregation reversal, at least for the systems investigated, are confirmed. In quantitative terms the PSM results prove useful only as estimates of the actual segregation state. On the other hand, it is probably unrealistic to expect that an essentially zero-dimensional model like the PSM be predictive when complex multiphase 3D CFD models still struggle to provide accurate simulations in this field.

From the point of view of applications, the possibility to design or govern the segregation direction of a fluid bed process, e.g. by selecting the inert size or amount, appears particularly attractive. Not only could one be able to include such effect right from the initial design of the operation and appropriate selection of relevant materials, but the improved understanding can also help preventing segregation-related problems. As an example, by designing a system to operate at the segregation equilibrium conditions, a straightforward result of the PSM, one should get a multi-component bed that tends to remain mixed right from the start of the fluidization process, i.e. even at very low superficial velocities, when segregation tendencies are typically stronger. Indeed, if high gas velocities are used to improve mixing (or contrast segregation) and are otherwise unnecessary, the present results open other possibilities to act upon in an attempt to bring the system at its critical segregation point while operating it at low velocities.

## **5. Conclusions**

The low-velocity fluidization characteristics of three binary mixtures were studied by model-guided experimentation with the aim to define the segregation tendency and check the occurrence of the segregation direction reversal with bed composition. The recently proposed Particle Segregation

Model (PSM), based on the concept of force balance on a particle immersed in a binary bed at minimum fluidization, was shortly summarized. Experiments were carried out to obtain the steady-state axial profiles of the fine solid volume fraction for mixtures composed of one cut of crushed olive pits (biomass), OP1540, and three different solids, glass ballotini, GB0250, and two sand cuts, SG0340 and SG0160. The inert sizes were selected in order to give the theoretically expected segregation direction reversal with bed composition, as predicted by the PSM. In all investigated cases the fluidized bed appeared relatively mixed, with the prevalence of layers of one or the other component often visible only at the bed surface. The modest segregation tendency exhibited in terms of the extracted composition profiles, however, allowed the prevailing phenomena to be quite clearly distinguished between, at least for most of the cases.

The main result of the present investigation is that the measurements of the axial volume fraction profiles confirmed the presence of a segregation reversal with bed composition for all the three systems. It should be noted that such phenomenon, as presented and discussed here, is essentially unreported for gas-fluidized beds in the literature.

Quantitative comparison of the observed vs. predicted critical compositions shows a different degree of agreement. For mixture A (GB0250-OP1540), a quite remarkable similitude is obtained between the value of the composition predicted at segregation equilibrium and the observed axial profiles, particularly when the dependence of the voidage with composition is taken into account. Observations of the segregation tendency exhibited by mixture B (SG0340-OP1540) show that the change of direction occurs approximately between volume fractions  $x_1 = 0.6$  and  $0.7$ . In contrast, the predicted critical value is only  $x_1 = 0.23$ . Mixture C (SG0160-OP1540) exhibits a quite unusual fluidization pattern, with the fluidization front propagating from the bottom to the top of the bed. This reflects in the concentration profiles that show a complex segregation tendency. Based on the shape of the profiles a segregation reversal point can be estimated at about  $x_1 = 0.7$ , to compare with the predicted value of  $x_1 = 0.4$ .

Overall, the predicting capability of PSM for the critical composition in quantitative terms can be judged satisfactory. However, the fact that a simple, first-principle and parameter-free model is able to capture the essence of a quite peculiar phenomenon for gas-fluidized beds represents a significant advancement of the theoretical tools available in the field.

## Notation

D	particle diameter, m
$\bar{D}$	Sauter's mean particle diameter, m
d	diameter ratio ( $D_1/D_2$ ), -
$\bar{d}$	average diameter ratio ( $\bar{D}/D_2$ ), -
F	pure drag force, N
g	gravitational acceleration, $m/s^2$
m	particle mass, kg
N	net fluid-particle interaction force, N
P	absolute pressure, Pa
p	net pressure, Pa
s	inverse density ratio ( $\rho_2/\rho_1$ ), -
$\bar{s}$	inverse average density ratio ( $\rho_2/\bar{\rho}$ ), -
u	gas superficial velocity, m/s
$u_{mf}$	minimum fluidization velocity, m/s
$\bar{u}_s$	gas superficial velocity at bed suspension, m/s
x	fluid-free solids volumetric fraction, -
y	polydispersion index $y_i = D_i/\bar{D}$ , -
W	total fluid-particle interaction force, N

## Greek letters

$\varepsilon$	voidage, -
---------------	------------

$\rho$	solid density, kg/m <sup>3</sup>
$\bar{\rho}$	average solid density, kg/m <sup>3</sup>

### Subscripts

0	packed bed
1, 2	index for solid species
eq	equilibrium
exp	experiments
i, j	relative to the i-th, or j-th particle or particle species
s	at suspension

## References

- [1] F.P. Di Maio, A. Di Renzo, V. Vivacqua, Extension and validation of the particle segregation model for bubbling gas-fluidized beds of binary mixtures, *Chem. Eng. Sci.* 97 (2013) 139–151. doi:10.1016/j.ces.2013.04.012.
- [2] H. Cui, J.R. Grace, Fluidization of biomass particles: A review of experimental multiphase flow aspects, *Chem. Eng. Sci.* 62 (2007) 45–55. doi:10.1016/j.ces.2006.08.006.
- [3] I. Aigner, C. Pfeifer, H. Hofbauer, Co-gasification of coal and wood in a dual fluidized bed gasifier, *Fuel*. 90 (2011) 2404–2412. doi:10.1016/j.fuel.2011.03.024.
- [4] Y.A. Alghamdi, E. Doroodchi, B. Moghtaderi, Mixing and segregation of binary oxygen carrier mixtures in a cold flow model of a chemical looping combustor, *Chem. Eng. J.* 223 (2013) 772–784. doi:10.1016/j.cej.2013.03.037.
- [5] T.J.P. Oliveira, C.R. Cardoso, C.H. Ataíde, Bubbling fluidization of biomass and sand binary mixtures: Minimum fluidization velocity and particle segregation, *Chem. Eng. Process. Process Intensif.* 72 (2013) 113–121. doi:10.1016/j.cep.2013.06.010.
- [6] Y. Zhang, B. Jin, W. Zhong, Experimental investigation on mixing and segregation behavior of biomass particle in fluidized bed, *Chem. Eng. Process. Process Intensif.* 48 (2009) 745–754. doi:10.1016/j.cep.2008.09.004.
- [7] F. Fotovat, J. Chaouki, J. Bergthorson, The effect of biomass particles on the gas distribution and dilute phase characteristics of sand–biomass mixtures fluidized in the bubbling regime, *Chem. Eng. Sci.* 102 (2013) 129–138. doi:10.1016/j.ces.2013.07.042.
- [8] P.N. Rowe, A.W. Nienow, A.J. Agbim, The Mechanisms by which Particles Segregate in Gas Fluidised Beds - Binary Systems of Near-Spherical particles, *Trans. Inst. Chem. Eng.* 50 (1972) 310–323.
- [9] L.G. Gibilaro, P.N. Rowe, A model for a segregating gas fluidised bed, *Chem. Eng. Sci.* 29 (1974) 1403–1412. doi:10.1016/0009-2509(74)80164-8.
- [10] P.N. Rowe, A.W. Nienow, Particle Mixing and Segregation in Gas Fluidised Beds. A Review, *Powder Technol.* 15 (1976) 141–147.
- [11] S.Y. Wu, J. Baeyens, Segregation by size difference in gas fluidized beds, *Powder Technol.* 98 (1998) 139–150. doi:10.1016/S0032-5910(98)00026-6.
- [12] L. Huilin, H. Yurong, D. Gidaspow, Y. Lidan, Q. Yukun, Size segregation of binary mixture of solids in bubbling fluidized beds, *Powder Technol.* 134 (2003) 86–97. doi:10.1016/S0032-5910(03)00126-8.
- [13] J. Gao, X. Lan, Y. Fan, J. Chang, G. Wang, C. Lu, et al., Hydrodynamics of gas–solid fluidized bed of disparately sized binary particles, *Chem. Eng. Sci.* 64 (2009) 4302–4316. doi:10.1016/j.ces.2009.07.003.
- [14] S.R. Dahl, C.M. Hrenya, Size segregation in gas–solid fluidized beds with continuous size distributions, *Chem. Eng. Sci.* 60 (2005) 6658–6673. doi:10.1016/j.ces.2005.05.057.

- [15] A.C. Hoffmann, L.P.B.M. Janssen, J. Prins, Particle segregation in fluidised binary mixtures, *Chem. Eng. Sci.* 48 (1993) 1583–1592. doi:10.1016/0009-2509(93)80118-A.
- [16] G.A. Bokkers, M. van Sint Annaland, J.A.M. Kuipers, Mixing and segregation in a bidisperse gas–solid fluidised bed: a numerical and experimental study, *Powder Technol.* 140 (2004) 176–186. doi:10.1016/j.powtec.2004.01.018.
- [17] J.W. Chew, J.R. Wolz, C.M. Hrenya, Axial segregation in bubbling gas-fluidized beds with Gaussian and lognormal distributions of Geldart Group B particles, *AIChE J.* 56 (2010) 3049–3061. doi:10.1002/aic.12219.
- [18] B. Formisani, R. Girimonte, T. Longo, The fluidization pattern of density-segregating binary mixtures, *Chem. Eng. Res. Des.* 86 (2008) 344–348. doi:10.1016/j.cherd.2007.11.004.
- [19] Y. Tatemoto, A. Ishii, Y. Suzuki, T. Higashino, Effect of Volume Fraction of Material on Separation by Density Difference in a Liquid-Fluidized Bed of Inert Particles, *Chem. Eng. Technol.* 33 (2010) 1169–1176. doi:10.1002/ceat.201000027.
- [20] B. Formisani, R. Girimonte, V. Vivacqua, Fluidization of mixtures of two solids: A unified model of the transition to the fluidized state, *AIChE J.* 59 (2013) 729–735. doi:10.1002/aic.13876.
- [21] B. Formisani, R. Girimonte, V. Vivacqua, Fluidization of mixtures of two solids differing in density or size, *AIChE J.* 57 (2011) 2325–2333. doi:10.1002/aic.12450.
- [22] G. Olivieri, A. Marzocchella, P. Salatino, Segregation of fluidized binary mixtures of granular solids, *AIChE J.* 50 (2004) 3095–3106. doi:10.1002/aic.10340.
- [23] A. Marzocchella, P. Salatino, V. Di Pastena, L. Lirer, Transient fluidization and segregation of binary mixtures of particles, *AIChE J.* 46 (2000) 2175–2182. doi:10.1002/aic.690461110.
- [24] A. Rao, J.S. Curtis, B.C. Hancock, C. Wassgren, Classifying the fluidization and segregation behavior of binary mixtures using particle size and density ratios, *AIChE J.* 57 (2011) 1446–1458. doi:10.1002/aic.12371.
- [25] G.G. Joseph, J. Leboeiro, C.M. Hrenya, A.R. Stevens, Experimental segregation profiles in bubbling gas-fluidized beds, *AIChE J.* 53 (2007) 2804–2813. doi:10.1002/aic.11282.
- [26] M.G. Rasul, V. Rudolph, M. Čársky, Segregation potential in binary gas fluidized beds, *Powder Technol.* 103 (1999) 175–181. doi:10.1016/S0032-5910(98)00230-7.
- [27] Y.Q. Feng, B.H. Xu, S.J. Zhang, A.B. Yu, P. Zulli, Discrete particle simulation of gas fluidization of particle mixtures, *AIChE J.* 50 (2004) 1713–1728. doi:10.1002/aic.10169.
- [28] L. Huilin, H. Yurong, D. Gidaspow, Hydrodynamic modelling of binary mixture in a gas bubbling fluidized bed using the kinetic theory of granular flow, *Chem. Eng. Sci.* 58 (2003) 1197–1205. doi:10.1016/S0009-2509(02)00635-8.
- [29] Y.Q. Feng, A.B. Yu, Microdynamic modelling and analysis of the mixing and segregation of binary mixtures of particles in gas fluidization, *Chem. Eng. Sci.* 62 (2007) 256–268. doi:10.1016/j.ces.2006.08.015.

- [30] L. Mazzei, A. Casillo, P. Lettieri, P. Salatino, CFD simulations of segregating fluidized bidisperse mixtures of particles differing in size, *Chem. Eng. J.* 156 (2010) 432–445. doi:10.1016/j.cej.2009.11.003.
- [31] A. Di Renzo, F.P. Di Maio, R. Girimonte, B. Formisani, DEM simulation of the mixing equilibrium in fluidized beds of two solids differing in density, *Powder Technol.* 184 (2008) 214–223. doi:10.1016/j.powtec.2007.11.031.
- [32] A. Di Renzo, F. Cello, F.P. Di Maio, Simulation of the layer inversion phenomenon in binary liquid–fluidized beds by DEM–CFD with a drag law for polydisperse systems, *Chem. Eng. Sci.* 66 (2011) 2945–2958. doi:10.1016/j.ces.2011.03.035.
- [33] B.P.B. Hoomans, J.A.M. Kuipers, W.P.M. van Swaaij, Granular dynamics simulation of segregation phenomena in bubbling gas–fluidised beds, *Powder Technol.* 109 (2000) 41–48. doi:10.1016/S0032-5910(99)00225-9.
- [34] M.A. Howley, B.J. Glasser, Hydrodynamics of a uniform liquid–fluidized bed containing a binary mixture of particles, *Chem. Eng. Sci.* 57 (2002) 4209–4226. doi:10.1016/S0009-2509(02)00361-5.
- [35] Z. Peng, E. Doroodchi, Y. Alghamdi, B. Moghtaderi, Mixing and segregation of solid mixtures in bubbling fluidized beds under conditions pertinent to the fuel reactor of a chemical looping system, *Powder Technol.* 235 (2013) 823–837. doi:10.1016/j.powtec.2012.11.047.
- [36] S. Chiba, A.W. Nienow, T. Chiba, H. Kobayashi, Fluidised binary mixtures in which the denser component may be flotsam, *Powder Technol.* 26 (1980) 1–10. doi:10.1016/0032-5910(80)85001-7.
- [37] R. Escudí, N. Epstein, J.R. Grace, H.T. Bi, Layer inversion phenomenon in binary–solid liquid–fluidized beds: Prediction of the inversion velocity, *Chem. Eng. Sci.* 61 (2006) 6667–6690. doi:10.1016/j.ces.2006.06.008.
- [38] R. Di Felice, Hydrodynamics Of Liquid Fluidisation, *Chem. Eng. Sci.* 50 (1995) 1213–1245.
- [39] L.G. Gibilaro, R. Di Felice, S.P. Waldram, P.U. Foscolo, A predictive model for the equilibrium composition and inversion of binary–solid liquid fluidized beds, *Chem. Eng. Sci.* 41 (1986) 379–387. doi:10.1016/0009-2509(86)87017-8.
- [40] M. Asif, Segregation velocity model for fluidized suspension of binary mixture of particles, *Chem. Eng. Process. Process Intensif.* 37 (1998) 279–286. doi:10.1016/S0255-2701(98)00034-8.
- [41] F.P. Di Maio, A. Di Renzo, V. Vivacqua, A particle segregation model for gas–fluidization of binary mixtures, *Powder Technol.* 226 (2012) 180–188. doi:10.1016/j.powtec.2012.04.040.
- [42] L.G. Gibilaro, *Fluidization dynamics*, Butterworth-Heinemann, 2001.
- [43] M.A. van der Hoef, R. Beetstra, J.A.M. Kuipers, Lattice-Boltzmann simulations of low-Reynolds-number flow past mono- and bidisperse arrays of spheres: results for the

permeability and drag force, *J. Fluid Mech.* 528 (2005) 233–254.  
doi:10.1017/S0022112004003295.

- [44] X. Yin, S. Sundaresan, Drag Law for Bidisperse Gas–Solid Suspensions Containing Equally Sized Spheres, *Ind. Eng. Chem. Res.* 48 (2009) 227–241. doi:10.1021/ie800171p.
- [45] F. Cello, A. Di Renzo, F.P. Di Maio, A semi-empirical model for the drag force and fluid–particle interaction in polydisperse suspensions, *Chem. Eng. Sci.* 65 (2010) 3128–3139. doi:10.1016/j.ces.2010.02.006.
- [46] X. Yin, S. Sundaresan, Fluid-particle drag in low-Reynolds-number polydisperse gas-solid suspensions, *AIChE J.* 55 (2009) 1352–1368. doi:10.1002/aic.11800.
- [47] L.W. Rong, K.J. Dong, A.B. Yu, Lattice-Boltzmann simulation of fluid flow through packed beds of spheres: Effect of particle size distribution, *Chem. Eng. Sci.* 116 (2014) 508–523. doi:10.1016/j.ces.2014.05.025.